Data-Driven control design by prediction error identification for a refrigeration system based on vapor compression

Daniel D. Huff, Gustavo R. Gonçalves da Silva and Lucíola Campestrini

Department of Automation and Energy, Universidade Federal do Rio Grande do Sul, Porto Alegre - RS, Brazil (e-mails: {daniel.huff,gustavo.rgs,luciola}@ufrgs.br)

Abstract: This paper deals with data-driven control design in a Model Reference (MR) framework for multivariable systems. Based on a batch of input-output data collected on the process, a fixed structure controller is estimated without using a process model, by embedding the control design problem in the Prediction Error (PE) identification of an optimal controller. A multivariable extension of the OCI (Optimal Controller Identification) method is applied in the design of PID controllers for a refrigeration system based on vapor compression, which is the subject of the benchmark process challenge of the IFAC PID 2018 conference. Simulation results show the obtained controllers perform significantly better than the ones provided by the benchmark challenge.

Keywords: Data-driven control, Model reference, OCI, MIMO systems, refrigeration system.

1. INTRODUCTION

Vapor compression is the leading technology worldwide in cooling generation, including air conditioning, refrigeration and freezing. A great deal of energy is required in such tasks and a fundamental issue is to design control strategies in order to increase the process efficiency (Rasmussen et al., 2005). Such efficiency is reached using a controller which satisfies tight performance requirements, such as zero steady-state error and fast transients.

High performance controllers are usually model-based, where a mathematical model representing the systems' dynamics should be derived. In the case of refrigeration systems, this model can be obtained through the principles of thermodynamics (see McKinley and Alleyne (2008), for instance) or through system identification. However, refrigeration systems present strong nonlinearities and high coupling, which make modeling or identification of such systems a hard task. In order to avoid this step, data-driven control methods (Bazanella et al., 2012) can be used: the controllers are designed based on one or more batches of data collected from the plant, without deriving a mathematical model for the process. The efficiency of such controllers depends on the collected data through an experiment, the controller structure and the definition of performance requirements.

Data-driven control methods are typically based on the Model Reference (MR) paradigm, in which the desired closed-loop performance is specified by means of a closed-loop transfer function – the Reference Model. There are several data-driven methods developed for single-input single-output (SISO) control problems in the literature. Some of them are iterative (Hjalmarsson et al., 1998; Karimi et al., 2004), others are "one-shot" – that is, non-iterative, as (Campi et al., 2002; Karimi et al., 2007) and Optimal Controller Identification (OCI) (Campestrini et al., 2017), which is the one employed in this work. However, SISO methods are not proper to be used when interactions between variables are significant, and some effort has been put in developing the extensions of these methods for the multiple-input multiple output (MIMO) case: extensions to iterative methodologies are presented in (Jansson and Hjalmarsson, 2004; Mišković et al., 2005) and have the disadvantage of requiring a higher number of experiments; the one-shots are presented in (Yubai et al., 2009; Formentin et al., 2012; Campestrini et al., 2016), which are based on only one experiment, or two in the case where instrumental variables are used.

The controller structure is an important choice in data-driven control design. This choice is to data-driven design as the model structure choice is to system identification (Ljung, 1999). However, it is common practice in data-driven control design, specially for the one-shot methods, to choose a controller that is linear in its parameters, which means that all the controller poles are fixed. An advantage of the OCI methodology (Campestrini et al., 2017) is that the controller structure can be chosen with a fixed part, in order to fix an integrator for example, and an identifiable transfer function, such that, besides zeros, poles can also be identified. This characteristic is explored in this work, where the derivative pole of a PID controller is not fixed, allowing better matching to the desired reference model.

In this paper a MIMO version of the OCI method is applied to the benchmark process challenge (Bejarano et al., 2017) of the IFAC PID 2018 conference. Both

⋆ This work was supported by CAPES and CNPq/BR.

decentralized and centralized PID are designed and the closed-loop performances obtained with such controllers are compared, through a combined criterion, to the ones obtained with the benchmark proposed controllers. Enhanced performances are obtained with both designed controllers.

The paper is organized as follows: Section 2 presents definitions and problem formulation. The OCI MIMO formulation is presented in Section 3. Section 4 presents the refrigeration system and Section 5 presents the simulations and obtained results. At last, conclusions are presented at the end of paper.

2. PRELIMINARIES

Consider a linear time-invariant discrete-time MIMO process

$$y(t) = G_0(q)u(t) + H_0(q)w(t), \tag{1}$$

where q is the forward-shift operator, $u(t)$ and $y(t)$ are n-vectors representing the process' input and output, respectively, and $w(t)$ is a sequence of independent random n-dimensional vectors with zero mean values and covariance matrix $E[w(t)w^T(t)] = \Lambda$. The transfer matrix $G_0(q)$ and the noise model $H_0(q)$ are square $n \times n$ matrices whose elements are proper rational transfer functions.

The design task is to tune the parameter vector $P \in \mathbb{R}^p$ of a linear time-invariant controller $C(q, P)$ in order to achieve a desired closed-loop response. We assume that this controller belongs to a given user-specified controller class $\mathcal{C}$ such that all elements of the loop transfer matrix $L(q) = G_0(q)C(q, P)$ have positive relative degree for all $C(q, P) \in \mathcal{C}$. The control action $u(t)$ can be written as

$$u(t) = C(q, P)e(t) = C(q, P)(r(t) - y(t)), \tag{2}$$

where $r(t)$ is the reference signal, which is assumed to be quasi-stationary and uncorrelated with the noise $w(t)$, that is, $\bar{E}\left[r(t)w^T(s)\right] = 0\ \forall t, s$, where

$$\bar{E}[f(t)] \triangleq \lim_{M\to\infty} \frac{1}{M}\sum_{t=1}^{M} E[f(t)]$$

with $E[\cdot]$ denoting expectation (Ljung, 1999). The system (1)-(2) in closed-loop becomes

$$y(t, P) = T(q, P)r(t) + (I - T(q, P))v(t), \tag{3}$$

$$T(q, P) = [I + G_0(q)C(q, P)]^{-1}G_0(q)C(q, P), \tag{4}$$

where $v(t) = H_0(q)w(t)$ and the dependence on the controller parameter vector P is now made explicit in the output signal $y(t, P)$.

The controller class $\mathcal{C}$ is defined as

$$\mathcal{C} = \{C(q, P) : P \in \mathcal{D}_P \subseteq \mathbb{R}^p\},$$

where the structure of the controller to be designed is defined as

$$C(q, P) = \begin{bmatrix} C_{11}(q, \rho_{11}) & C_{12}(q, \rho_{12}) & \cdots & C_{1n}(q, \rho_{1n}) \\ \vdots & \vdots & \ddots & \vdots \\ C_{n1}(q, \rho_{n1}) & C_{n2}(q, \rho_{n2}) & \cdots & C_{nn}(q, \rho_{nn}) \end{bmatrix} \tag{5}$$

and $P = [\rho_{11}^T \ \ \rho_{12}^T \ \ \ldots \ \ \rho_{n1}^T \ \ \ldots \ \ \rho_{nn}^T]^T$. A particularly relevant class, which will be used in this paper, is that of Proportional-Integral-Derivative (PID) controllers with free derivative pole. In such PID controllers each nonzero element of the controller matrix $C(q, P)$ in (5) has the following parametrized structure

$$C_{ij}(q, \rho_{ij}) = \frac{a_{ij}q^2 + b_{ij}q + c_{ij}}{(q-1)(q-d_{ij})} \tag{6}$$

where $\rho_{ij} = [a_{ij} \ \ b_{ij} \ \ c_{ij} \ \ d_{ij}]^T$.

In the Model Reference approach to the design, the closed-loop performance is specified through the desired closed-loop transfer matrix $T_d(q)$, also known as the *reference model*. The controller parameters are then tuned as the solution of the problem

$$\hat{P}^{MR} = \arg\min_{P} \ \ J^{MR}(P), \tag{7}$$

$$J^{MR}(P) \triangleq \frac{1}{M}\sum_{t=1}^{M} ||(T_d(q) - T(q, P))r(t)||_2^2, \tag{8}$$

where $r(t)$ is the reference signal of interest and M is the time horizon.

The *ideal controller* $C_d(q)$ is the one that allows the closed-loop system behavior to match exactly the one prescribed by $T_d(q)$ and is given by

$$C_d(q) = G_0(q)^{-1}T_d(q)[I - T_d(q)]^{-1}. \tag{9}$$

If (9) were used in the closed-loop, then the objective function (8) would evaluate to zero. However, this ideal controller may not correspond to any controller in the controller set $\mathcal{C}$; actually in most practical applications it will not belong to $\mathcal{C}$. When considering the situation where $C_d(q) \in \mathcal{C}$, we shall say that the following assumption holds:

Assumption 1. Matching condition

$$\exists\ P_d \in \mathcal{D}_P \ \text{ such that } \ C(q, P_d) = C_d(q).$$

Achieving this condition for a predefined controller structure requires a proper choice of the reference model, which in turn requires some prior knowledge of the process (Bazanella et al., 2012; Gonçalves da Silva et al., 2014).

3. OPTIMAL CONTROLLER IDENTIFICATION

Using the concept of the ideal controller, it is possible to turn the model reference control design problem into an identification problem of the controller, without using a model for the process. This data-driven design method was presented in (Campestrini et al., 2017) for SISO systems and a MIMO version is used in this work. We now briefly describe the method.

The core idea is to rewrite the input-output system (1) in terms of the ideal controller $C_d(q)$, which is done by inverting the relation (9), i.e.,

$$G_0(q) = T_d(q)\left(I - T_d(q)\right)^{-1} C_d^{-1}(q). \tag{10}$$

Then a model for the plant can be written in terms of the controller parameters as

$$G(q, P) \triangleq T_d(q)\left(I - T_d(q)\right)^{-1} C^{-1}(q, P) \tag{11}$$

and the task will be to identify a model $C(q, \hat{P})$ of the ideal controller $C_d(q)$ within the parametrized controller class defined by $\mathcal{C}$. In other words, this corresponds to an identification of a plant model $G(q, P)$ with a fixed part,

which is a function of the reference model $T_d(q)$, and a parametrized part, which is a function of the controller inverse. Thus, (1) can be rewritten as

$$y(t,\Theta) = G(q,P)u(t) + H(q,\Theta)w(t) \tag{12}$$

where $\Theta = \begin{bmatrix} P^T & Q^T \end{bmatrix}^T$ and $Q \in \mathbb{R}^c$ is an additional parameter vector that appears in the noise model.

From M measured input-output data, the parameter vector estimate $\hat{\Theta}_M = \begin{bmatrix} \hat{P}_M^T & \hat{Q}_M^T \end{bmatrix}^T$ is defined as (Campestrini et al., 2017):

$$\hat{\Theta}_M = \arg\min_{\Theta} V(\Theta) \tag{13}$$

$$V(\Theta) = \frac{1}{M}\sum_{t=1}^{M} \|\epsilon(t,\Theta)\|_2^2, \tag{14}$$

where $\epsilon(t,\Theta)$ is the prediction error

$$\epsilon(t,\Theta) \triangleq y(t) - \hat{y}(t|t-1,\Theta) \tag{15}$$

and

$$\hat{y}(t|t-1,\Theta) = H^{-1}(q,\Theta)T_d(q)\left(I - T_d(q)\right)^{-1} C(q,P)^{-1}u(t) + \left[I - H^{-1}(q,\Theta)\right] y(t) \tag{16}$$

is the one-step ahead predictor for model (12), where $G(q,P)$ has been replaced by (11). The predictor is now a function of the inverses of the noise model and the controller.

Instead of minimizing $J^{MR}(P)$, which depends on the unknown plant $G_0(q)$, the design is made by minimizing the cost function $V(\Theta)$, which is purely data-dependent and no model of the plant $G_0(q)$ is used. Since the estimation of the optimal MR controller has been transformed into a PE identification problem, all properties of PE identification theory apply. Specifically, the estimate in (13) converges to the vector $\Theta^* = \begin{bmatrix} P^{*T} & Q^{*T} \end{bmatrix}^T$ defined as:

$$\hat{\Theta}_M \to \Theta^* = \arg\min_{\Theta} \bar{V}(\Theta) \tag{17}$$

where

$$\bar{V}(\Theta) = \bar{E}\,\|\epsilon(t,\Theta)\|_2^2. \tag{18}$$

It is worth mentioning that, since the object of interest is the optimal controller only, and not the plant model, the identification of $H_0(q)$ is of no interest for the controller design. It is well known from PE identification theory that if the real system belongs to the chosen model class (Assumption 1 is satisfied, in the controller identification problem), an informative enough data set is collected in open loop, and $G(q,P)$ and $H(q,\Theta)$ are parametrized independently (that is, $\frac{\partial H(q,\Theta)}{\partial P} = 0$), then, for $M \to \infty$ (Ljung, 1999):

$$C(q,\hat{P}_M) \to C_d(q). \tag{19}$$

If Assumption 1 is satisfied but data are collected in closed-loop, then (19) holds provided that $\exists\Theta_0$ such that $H(q,\Theta_0) = H_0(q)$.

It is often the case that one imposes some fixed part in the controller, the most common instance of this fact probably being the imposition of a pole at $q = 1$ to guarantee zero steady-state error for constant references and perturbations. This fixed part does not need to be identified. So, we call $C_F(q)$ this fixed *scalar* part and rewrite the controller transfer function as

$$C(q,P) = C_F(q)C_I(q,P). \tag{20}$$

Using (20) and (11), (12) can be written as

$$y(t,\Theta) = \underbrace{T_d(q)\left(I - T_d(q)\right)^{-1} C_F^{-1}(q)}_{F(q)} \underbrace{C_I^{-1}(q,P)}_{\tilde{C}(q,P)} u(t) + H(q,\Theta)w(t) \tag{21}$$

where $F(q)$ is a fixed transfer matrix formed by the fixed part of $G(q,P)$. In the noise-free scenario, *which is the case of the benchmark simulations*, we consider $H(q,\Theta) = I$ and the predictor (16) is reduced to

$$\hat{y}(t|t-1,P) = F(q)\tilde{C}(q,P)u(t). \tag{22}$$

Also, notice that in the SISO case, $F(q)$ commutes with $\tilde{C}(q,P)$ and (21) can be written as

$$\begin{aligned} y(t,\Theta) &= \underbrace{C_I^{-1}(q,P)}_{\tilde{C}(q,P)} \times \underbrace{T_d(q)\left(I - T_d(q)\right)^{-1} C_F^{-1}(q)u(t)}_{\tilde{u}(t)} + H(q,\Theta)w(t) \\ &= \tilde{C}(q,P)\tilde{u}(t) + H(q,\Theta)w(t). \end{aligned} \tag{23}$$

Solution for (23) can be easily obtained through available toolboxes like Matlab® `ident`. However, in the MIMO case the matrices in (21) do not commute. Thus a dedicated optimization solution was implemented in order to minimize (14), using the Matlab® function `fminunc`. This algorithm requires an initial controller parameter vector, which was obtained through the application of the MIMO version of Virtual Reference Feedback Tuning (VRFT) (Campestrini et al., 2016), a one-shot data-driven method.

4. REFRIGERATION SYSTEM

As mentioned above, the OCI method will be used to design PID controllers for a refrigeration system proposed by the benchmark PID 2018 (Bejarano et al., 2017). A canonical one-compression-stage, one-load-demand vapor-compression refrigeration cycle is shown in Figure 1, where the main components are represented.

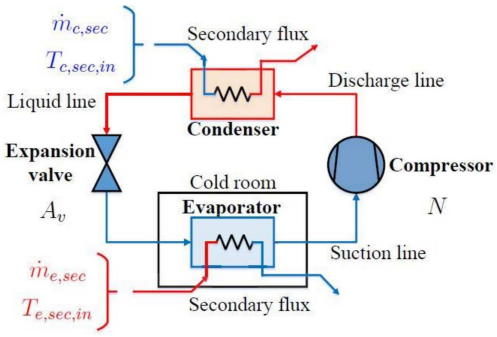

Fig. 1. Schematic picture of one-compression-stage, one-load-demand vapor-compression refrigeration cycle.

The inverse Rankine cycle is applied, where the refrigerant, R404a, removes heat from the secondary flux at the evaporator, which is a 60% propylene glycol aqueous solution, and reject heat at the condenser by transferring it to its secondary flux (air). The compressor is responsible for increasing the refrigerant pressure and temperature

while the expansion valve upholds the pressure difference between the condenser and the evaporator (Bejarano et al., 2017).

The variables to be controlled are the outlet temperature of the evaporator secondary flux $T_{e,sec,out}$ and the degree of superheating of the refrigerant at the evaporator outlet T_{SH}, but their desired values cannot be set independently. The manipulated variables are the compressor speed N and the expansion valve opening A_v. Besides that, Table 1 shows some variables that act as measurable disturbances.

Table 1. System disturbances.

Disturbance	Symbol	Unit
Inlet temperature of the condenser secondary flux	$T_{c,sec,in}$	°C
Mass flow of the condenser secondary flux	$\dot{m}_{c,sec}$	g/s
Inlet pressure of the condenser secondary flux	$P_{c,sec,in}$	bar
Inlet temperature of the evaporator secondary flux	$T_{e,sec,in}$	°C
Mass flow of the evaporator secondary flux	$\dot{m}_{e,sec}$	g/s
Inlet pressure of the evaporator secondary flux	$P_{e,sec,in}$	bar
Compressor surroundings temperature	T_{surr}	°C

The designed PID controllers will be compared to the ones proposed by the benchmark. One of them is a multivariable PID controller (whose gains are omitted), while the other is a decentralized one, which is shown below:

$$C(q) = \begin{bmatrix} \frac{-1.0136(q-1.0240)(q+0.9623)}{(q-1)(q-0.9853)} & \cdots \\ 0 & \end{bmatrix} \cdots \begin{bmatrix} 0 \\ \frac{0.42(q-0.04762)}{q-1} \end{bmatrix}. \quad (24)$$

In this last case, the outlet temperature of the evaporator secondary flux is controlled by means of the expansion valve, while the compressor speed controls the degree of superheating. All the controllers mentioned are in the discrete-time domain, while the sampling time is considered to be $T_s = 1$s.

Closed-loop performance is evaluated through eight individual indices and one combined index, as explained in the benchmark documentation (Bejarano et al., 2017). The first two indices are the Ratios of Integrated Absolute Error (RIAE), taking into account that both plant outputs ($T_{e,sec,out}$ and T_{SH}, in this order) should follow their respective references. The third is the Ratio of Integrated Time multiplied Absolute Error (RITAE) for $T_{e,sec,out}$, which penalizes the tracking error according to the time elapsed since the instant of reference change. The fourth, fifth, and sixth indices are the Ratios of Integrated Time multiplied Absolute Error (RITAE) for T_{SH} (considering three different step changes in its reference). The seventh and eighth indices are the Ratios of Integrated Absolute Variation of Control signal (RIAVU) for the two manipulated variables, which penalize the time derivative of A_v and N (in this order). The combined index corresponds to a weighted average of the eight individual indices. An index smaller than 1 means the controller C_2 is better than C_1 (see tables presented on next section).

5. SIMULATION RESULTS

The system is always simulated considering the initial operating point given in Table 2. In order to collect data from

Table 2. Initial operating point.

Variable		Value	Unit
Manipulated variables	A_v	48.79	%
	N	36.45	Hz
Disturbances	$T_{c,sec,in}$	30	°C
	$\dot{m}_{c,sec}$	150	g/s
	$P_{c,sec,in}$	1	bar
	$T_{e,sec,in}$	−20	°C
	$\dot{m}_{e,sec}$	64.503	g/s
	$P_{e,sec,in}$	1	bar
	T_{surr}	25	°C
Output variables	$T_{e,sec,out}$	−22.15	°C
	T_{SH}	14.65	°C

the system to apply the OCI method, the experiment is set as follows: the system starts at the given initial conditions and the input is set as a Pseudorandom Binary Sequence (PRBS) with fundamental period of 20 samples (the sampling time is $T_s = 1$s) and amplitudes ±10% for the valve opening and ±5 Hz for the compressor speed, plus their initial conditions. It is assumed that the disturbances remain constant through the whole experiment, which can be considered true if the surroundings' temperature and pressure do not vary and if there are no load changes at the refrigerator during the 20min of experiment. The result is portrayed in Fig. 2.

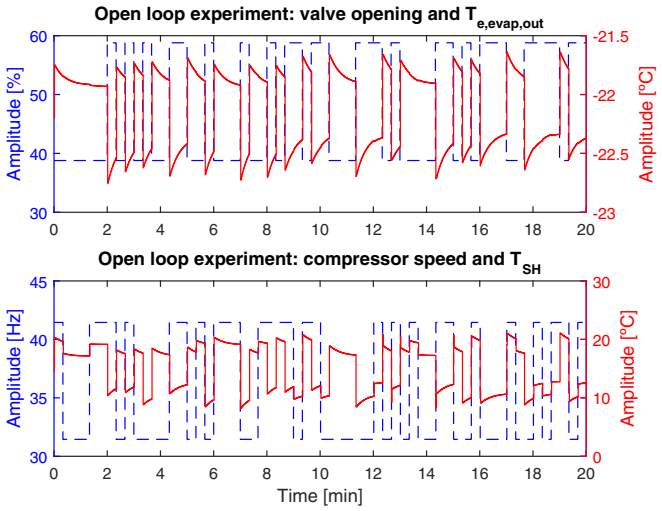

Fig. 2. PRBS open-loop experiment with all disturbances kept constant.

With this batch of data both a decentralized and a centralized PID controller were designed for the following reference model:

$$T_d(q) = \frac{0.9}{q-0.1} I_2, \quad (25)$$

where I_2 is the identity matrix of size 2. The chosen $T_d(q)$ corresponds to a settling time of 2s and zero steady-state error for step references (Gonçalves da Silva et al., 2014).

Using the collected data presented in Fig. 2 and (25), the MIMO VRFT method was applied to obtain the initial controllers for OCI. Both a decentralized and a centralized controller were obtained, given, respectively, by

$$C(q) = \begin{bmatrix} \frac{-23.4(q^2+0.01057q+0.0142)}{q(q-1)} & \cdots \\ 0 & \end{bmatrix} \begin{matrix} 0 \\ \frac{0.224(q-0.09652)(q-0.03344)}{q(q-1)} \end{matrix} \quad (26)$$

$$C(q) = \begin{bmatrix} \frac{-21.70(q-0.0644)(q+0.0600)}{q(q-1)} & \cdots \\ \frac{-45.79(q-0.0294)(q+0.0282)}{q(q-1)} & \end{bmatrix} \begin{matrix} \frac{-0.1522(q^2+0.2052q+0.2384)}{q(q-1)} \\ \frac{4.0591(q-0.0890)(q+0.0819)}{q(q-1)} \end{matrix} \quad (27)$$

The combined performance index $\mathrm{J}(C_2, C_1)$ obtained with the initial controllers is given in Table 3. The enhancement already obtained with the VRFT controller is visible: compared to the given decentralized controller (24) both designs presented a smaller cost, while when comparing to the MIMO benchmark controller, the centralized VRFT controller was able to provide a smaller cost.

Table 3. Combined indices of VRFT controllers compared to provided controllers.

	Comparing to (24)		Comparing to MIMO	
	C_2 =(26)	C_2 =(27)	C_2 =(26)	C_2 =(27)
$\mathrm{J}(C_2, C_1)$	0.656	0.317	2.004	0.506

The VRFT decentralized controller (26) was used as initial condition to design the decentralized OCI controller, while (27) was used as initial condition to the centralized design. The obtained OCI controllers are:

$$C(q) = \begin{bmatrix} \frac{-23.3(q^2+0.007902q+0.02767)}{(q-1)(q-0.1227)} & \cdots \\ 0 & \end{bmatrix} \begin{matrix} 0 \\ \frac{5.548(q^2+0.0839q+0.05338)}{(q-1)(q+0.1078)} \end{matrix} \quad (28)$$

$$C(q) = \begin{bmatrix} \frac{-22.48(q+0.0562)(q-0.9558)}{(q-0.9652)(q-1)} & \cdots \\ \frac{-46.35(q+0.02822)(q-0.04973)}{(q-0.08749)(q-1)} & \end{bmatrix} \begin{matrix} \frac{-0.1023(q^2-1.788q+0.9597)}{(q-1)(q-0.9834)} \\ \frac{4.098(q+0.05817)(q-0.9831)}{(q-0.9762)(q-1)} \end{matrix} \quad (29)$$

Taking into account the ranges of the manipulated variables, which are $10-100\%$ for A_v and $30-50$ Hz for N, the backtracking anti-windup technique (Peng et al., 2015) was implemented in order to improve the controllers performance. Fig. 3 shows the block diagram related to the compressor speed, where $\hat{N}$ is its desired value and N is the real one, which is applied to the system. A similar reasoning applies to the valve opening. The gain k of the anti-windup loop was chosen equal to 0.8.

Figs. 4 and 5 show the plant inputs and outputs, respectively, obtained with both OCI controllers compared to the provided results of the given MIMO controller, with unknown transfer function. This controller is named as *Base MIMO* controller in comparisons. In this simulation, the value of the disturbance $T_{e,sec,in}$ switches from $-20\,^{\circ}\mathrm{C}$ to $-21\,^{\circ}\mathrm{C}$ at the time instant $t = 9$ min and from $-21\,^{\circ}\mathrm{C}$ to $-20\,^{\circ}\mathrm{C}$ at $t = 16$ min. Moreover, $T_{c,sec,in}$ switches from $30\,^{\circ}\mathrm{C}$ to $27\,^{\circ}\mathrm{C}$ at $t = 16$ min. The other disturbances remain at their initial values.

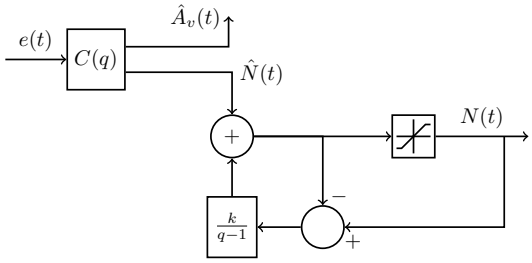

Fig. 3. Backtracking anti-windup technique.

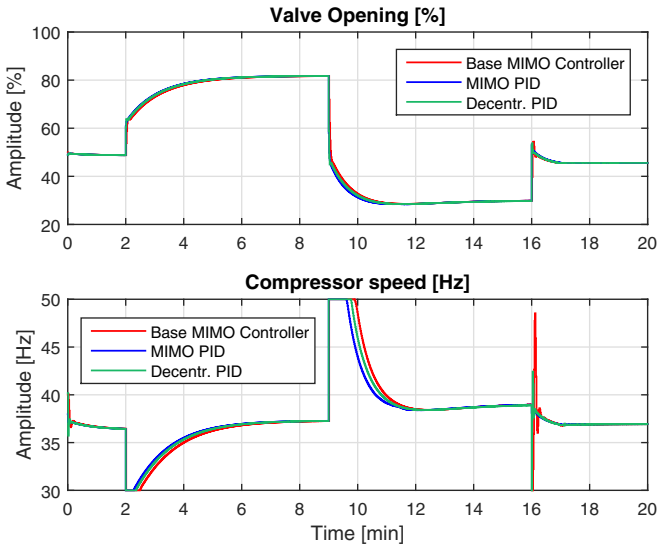

Fig. 4. Inputs of the closed-loop experiment in the proposed scenario.

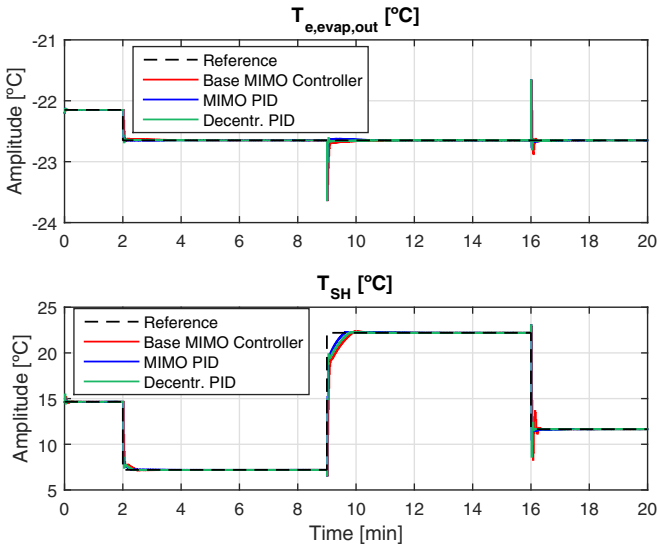

Fig. 5. Outputs of the closed-loop experiment in the proposed scenario.

As it can be seen in Figs. 4 and 5, closed-loop response with the designed controllers is visually slightly better than the original one. Table 4 shows that the improvement is actually relevant. It compares the OCI controllers to the Base MIMO controller and also to the one in (24).

Notice that the combined performance indices related to the OCI controllers (last row of Table 4) are smaller

Table 4. R_{indices} and J compared to provided controllers.

	Comparing to (24)		Comparing to MIMO	
	C_2 =(28)	C_2 =(29)	C_2 =(28)	C_2 =(29)
RIAE_1	0.1406	0.1589	0.4005	0.4526
RIAE_2	0.2515	0.221	0.5642	0.4958
RITAE_1	0.5444	0.0655	0.338	0.04071
RITAE_2	0.0708	0.05062	0.387	0.2767
RITAE_3	0.1901	0.1911	0.5948	0.5979
RITAE_4	0.03556	0.09228	0.2777	0.7207
RIAVU_1	1.13	1.096	1.002	0.9711
RIAVU_2	1.243	0.6714	0.905	0.4887
$\text{J}(C_2, C_1)$	0.3225	0.1844	0.4576	0.4074

(some by a factor of ≈ 2 or more) than the ones related to the VRFT controllers, which are shown in Table 3. This is mainly due to the fact that the derivative pole is considered free in OCI and fixed in VRFT.

At last, Table 5 compares the designed OCI controllers between them. Notice that the centralized controller has a better overall performance ($\text{J}(C_2, C_1) < 1$), but the decentralized one is also suitable for practical purposes.

Table 5. R_{indices} and J between proposed controllers.

	C_1 =(28) and C_2 =(29)
RIAE_1	1.13
RIAE_2	0.8788
RITAE_1	0.1204
RITAE_2	0.7149
RITAE_3	1.005
RITAE_4	2.595
RIAVU_1	0.9693
RIAVU_2	0.54
$\text{J}(C_2, C_1)$	0.938

6. CONCLUSIONS

A MIMO version of the OCI method was applied to the benchmark process. No process model is obtained and the designed PID controllers provided better results than the original ones. The anti-windup technique employed also contributes to improving closed-loop performance.

Compared to the provided benchmark controllers, the designed ones with the OCI method resulted in smaller costs. The only exception concerns the performance indices related to the manipulated variables, for which costs smaller than 1 were achieved in half of the comparisons made, even though the combined cost is always smaller. Compared to the initial VRFT controllers, the OCI ones also resulted in smaller combined costs. This fact can be explained considering the derivative pole of the PIDs, which is fixed in VRFT and free in OCI. In other words, the controller structure has more degrees of freedom, allowing an identification closer to the matching condition.

REFERENCES

Bazanella, A.S., Campestrini, L., and Eckhard, D. (2012). *Data-driven Controller Design: The H_2 Approach*. Springer, Netherlands.

Bejarano, G., Alfaya, J.A., Rodríguez, D., Ortega, M.G., and Morilla, F. (2017). *Benchmark for PID control of Refrigeration Systems based on Vapour Compression*.

Campestrini, L., Eckhard, D., Bazanella, A.S., and Gevers, M. (2017). Data-driven model reference control design by prediction error identification. *Journal of the Franklin Institute*, 354(6), 2828–2647.

Campestrini, L., Eckhard, D., Chía, .A., and Boeira, E. (2016). Unbiased MIMO VRFT with application to process control. *Journal of Process Control*, 39, 35–49.

Campi, M., Lecchini, A., and Savaresi, S. (2002). Virtual reference feedback tuning: a direct method for the design of feedback controllers. *Automatica*, 38, 1337–1346.

Formentin, S., Savaresi, S., and del Re, L. (2012). Non-iterative direct data-driven controller tuning for multivariable systems: theory and application. *Control Theory Applications, IET*, 6(9), 1250–1257.

Gonçalves da Silva, G.R., Campestrini, L., and Bazanella, A.S. (2014). Automating the choice of the reference model for data-based control methods applied to PID controllers. In *XX Congresso Brasileiro de Automática*, 1088–1095. SBA, Belo Horizonte.

Hjalmarsson, H., Gevers, M., Gunnarsson, S., and Lequin, O. (1998). Iterative feedback tuning: theory and applications. *IEEE Control Systems Magazine*, 18(4), 26–41.

Jansson, H. and Hjalmarsson, H. (2004). Gradient approximations in iterative feedback tuning for multivariable processes. *International Journal of Adaptive Control and Signal Processing*, 18(8), 665–681.

Karimi, A., Mišković, L., and Bonvin, D. (2004). Iterative correlation-based controller tuning. *International Journal of Adaptive Control and Signal Processing*, 18, 645–664.

Karimi, A., van Heusden, K., and Bonvin, D. (2007). Noniterative data-driven controller tuning using the correlation approach. In *European Control Conference 2007*, 5189–5195.

Ljung, L. (1999). *System Identification: Theory for the User*. Prentice-Hall, 2^{nd} edition.

McKinley, T.L. and Alleyne, A.G. (2008). An advanced nonlinear switched heat exchanger model for vapor compression cycles using the moving-boundary method. *International Journal of Refrigeration*, 31(7), 1253–1264.

Mišković, L., Karimi, A., Bonvin, D., and Gevers, M. (2005). Correlation-based tuning of linear multivariable decoupling controllers. In *Decision and Control, 2005 and 2005 European Control Conference. CDC-ECC '05. 44th IEEE Conference on*, 7144–7149.

Peng, Y., Vrancic, D., and Hanus, R. (2015). Anti-windup, bumpless, and conditioned transfer techniques for PID controllers. *IEEE International Conference on Industrial Technology*.

Rasmussen, B.P., Museer, A., and Alleyne, A.G. (2005). Model-driven system identification of transcritical vapor compression systems. *IEEE Transactions on Control Systems Technology*, 13, 444–451.

Yubai, K., Usami, H., and Hirai, J. (2009). Correlation-based direct tuning of MIMO controllers by least-squares and its application to tension-and-speed control apparatus. In *ICCAS-SICE, 2009*, 931–936.